Environ Sci Pollut Res (2017) 24:9468–9480
DOI 10.1007/s11356-017-8518-3

RESEARCH ARTICLE

Evaluation of black crust formation and soiling process on historical buildings from the Bilbao metropolitan area (north of Spain) using SEM-EDS and Raman microscopy

Estefanía Calparsoro[1] · Maite Maguregui[2] · Anastasia Giakoumaki[3] · Héctor Morillas[3] · Juan Manuel Madariaga[3]

Received: 14 September 2016 / Accepted: 30 January 2017 / Published online: 24 February 2017

Abstract In the present work, several building materials suffering from black crusts and soiled surfaces were evaluated by scanning electron microscopy energy dispersive X-ray spectrometry (SEM-EDS) and micro-Raman spectroscopy. The goal was to examine the elemental and molecular composition, the distribution on the samples, and the morphology of endogenous and exogenous compounds on those black crusts and soiled surfaces. The black crusts were deposited over different building materials such as limestone, sandstone, and brick that constitute a small construction called "malacate" as well as over a limestone substrate of a cemetery gate. Both constructions are dated back to the beginning of the twentieth century. The samples of soiling were taken from the façade of a building constructed in the 1980s. The analytical evaluation allowed in a first stage the determination of the composition and the observation of the morphology of soiling and black crusts. In addition, the evaluation of the compositions of the soiling and black crusts of different grade and formation allowed the assessment of the main weathering phenomena that the buildings have suffered, which were found to be sulfate impact, marine aerosol impact, depositions of metallic particles, crustal particulate matter depositions, carbonaceous particles, biodeterioration, and vandalism.

Keywords Black crust · Soiling · Greenhouse acid gases · Raman microscopy · SEM-EDS · Bilbao metropolitan area historical buildings

Responsible editor: Michel Sablier

Electronic supplementary material The online version of this article (doi:10.1007/s11356-017-8518-3) contains supplementary material, which is available to authorized users.

✉ Maite Maguregui
maite.maguregui@ehu.es

[1] Department of Geography, History and Archaeology, Faculty of Arts, University of the Basque Country UPV/EHU, 01006 Vitoria-Gasteiz, Basque Country, Spain

[2] Department of Analytical Chemistry, Faculty of Pharmacy, University of the Basque Country UPV/EHU, P.O. Box 450, 01080 Vitoria-Gasteiz, Basque Country, Spain

[3] Department of Analytical Chemistry, Faculty of Science and Technology, University of the Basque Country UPV/EHU, P.O. Box 644, 48080 Bilbao, Basque Country, Spain

Introduction

The majority of heritage constructions are constituted by stone and brick materials. Their outdoor character makes them vulnerable to the atmospheric weathering phenomena (Doehne and Price 2011) and, among the effects likely to occur, the formation of black crusts and soiling are of special importance, apart from the blackening of the surfaces (Brimblecombe and Grossi 2005), because they lead to physicochemical decay and also act as a pollutant accumulator (Schiavon et al. 2004; Larssen et al. 2006; Charola et al. 2007; Barca et al. 2010; Barca et al. 2014; Ruffolo et al. 2015) and acting in some cases as natural passive samplers (Morillas et al. 2016a). Consequently, not only they suppose an aesthetical problem, but in some cases they can also jeopardize the integrity of a construction. In addition, these crusts are prone to include or accumulate diverse microorganisms and organic compounds in its structure. Some of these microorganism can biosynthesize large amounts of hydrated calcium oxalate (McAlister et al. 2008) or even also promote a physical stress on the building material (cracks, fissures, etc.) placed at the back of the crust. In fact, it has already been reported that the accumulation of organic pollutants leads to an increase of microorganism activity (Potgieter-Vermaak et al. 2005).

Black crust growth is due to the formation of gypsum on surfaces sheltered from water and attacked by SO_2-polluted atmosphere. According to the International Council on Monuments and Sites (ICOMOS) glossary (ICOMOS 2008), black crust is a "Kind of crust developing generally on areas protected against direct rainfall or water runoff in urban environment. They are composed mainly of particles from the atmosphere, trapped into a gypsum matrix ($CaSO_4 \cdot 2H_2O$)." On the other hand, soiling is a "Deposit of a very thin layer of exogenous particles (e.g. soot) giving a dirty appearance to the stone surface. […] With increasing adhesion and cohesion, soiling can transform into a crust" (ICOMOS 2008).

The identification of the particulate matter deposited on stone/brick surfaces plays a crucial role in the understanding of the type of weathering processes suffering or likely to be suffered by this kind of substrates (Maguregui et al. 2008). At the same time, they provide significant information about the surrounding atmosphere, reflecting indirectly the air quality, which has an important effect in the environment as well as in the human health.

The nature of the inorganic salt crystallization occurring in the black crusts and soiling has been widely studied. Works on the field focused on the study of carbon and metallic particle depositions, and on the characterization of the nature of metallic particles deposited on black crust are increasing in the last years (Sýkorová et al. 2011; Ruffolo et al. 2015; Morillas et al. 2016a).

The present work reports a detailed microscopic and chemical characterization of different altered stone and brick surfaces to shed light on the deterioration mechanisms happening on heritage buildings due to the influence of urban polluted and coastal environments.

Regarding the analytical techniques used in the field of building material analysis, non-invasive techniques based on micro-spectroscopy have gained ground in the last years. It is especially an important development carried out in the spectral mapping techniques for the application on building materials that have suffered impact of atmospheric pollution such as the following spectroscopic techniques: Raman spectroscopy, infrared spectroscopy, micro-X-ray fluorescence spectrometry, scanning electron microscopy coupled to energy dispersive X-ray spectrometry (SEM-EDS), laser ablation inductively coupled plasma mass spectrometry (LA-ICP-MS), etc. (Watson et al. 2005; Sarmiento et al. 2008; Barca et al. 2010; Barca et al. 2011; Crupi et al. 2016; Morillas et al. 2016b; Morillas et al. 2016c). Although such techniques are commonly used in a non-quantitative way, they allow determining the conservation state of the materials under study in a first stage.

For this study, (SEM-EDS) and micro-Raman spectroscopy were chosen because they allow obtaining the elemental and molecular composition of the compounds embedded inside the crust. They also allow visualizing the black crust appearance as well as the surfaces that have suffered soiling processes. Furthermore, both techniques allow a micro-invasive characterization of small samples. Moreover, by Raman spectroscopy, it is possible to discern between different calcium sulfate polymorphs depending on their hydration states such as gypsum or anhydrite, which are of special relevance concerning the degradation processes that their dissolution/precipitation cycles may imply (Rodríguez-Navarro et al. 2000; Flatt 2002; Espinosa-Marzal and Scherer 2010). The use of micro-spectroscopic techniques for the study of this type of damaged layers has had an increase in the last years since it provides reliable information about their composition.

In the present work, black crusts formed on sandstone, limestone, and brick substrates belonging to one-century-old constructions were sampled, as well as soiling samples from an approximately 30-year-old building façade. All these historical buildings are located in the metropolitan area of Bilbao (Basque Country, north of Spain). As mentioned above, for the sample characterization, SEM-EDS and micro-Raman spectroscopy techniques were selected.

Materials and methods

Sampling

All the studied cases are from buildings located in the municipality of Getxo (Biscay, north of Spain), which belongs to the metropolitan area of Bilbao (Basque Country, north of Spain). The sites are in an architecturally noteworthy area situated on the coast, where the Nerbioi-Ibaizabal estuary finishes. This estuary is the major industrialized area with the highest population density of the north of Spain. Due to its geographic situation and because of its mineral resource richness, mainly iron, since the nineteenth century, this area has suffered the rapid growth of industrialization and population developments with the subsequent pollution problems. These problems were mainly manifested since the 1930s, but it was not until after the 1960s, when the inhabitants started to be aware of them. Despite the improvement of the environmental conditions, the high rates of air pollution during this period are still obvious in many building surfaces of the area. In order to study if signs of this pollution are evident on different kind of crusts formed on buildings, two historical buildings and a more recent one were selected. In total, 15 samples have been considered for this work. All the samples have been taken at around 1–1.5 m from the ground level.

Malcate building

This small construction (built around 1900) is one of the remaining constructions that were built to control the sewage system of Bilbao, as part of the first modern sewage network of the state. It was a necessary infrastructure for the rapidly growing industrial society. It was built with rich architectural elements, in terms of materials and structure. In 1994, the malacate buildings were designated monumental sets of the Basque Country, and in 2004, this specific malacate building located in the municipality of Getxo was included inside the list of historic and architectural heritage properties from the Basque Country. This building presents black crusts on sheltered areas of the three materials used for its construction: limestone, sandstone, and brick (see Fig. 1b). All these materials covered with black crust were sampled for this work. From each material showing the presence of black crusts, three fragments, a biggest one (around 3 × 3 cm) and two smallest fragments (around 0.5 × 0.5 cm), were taken.

The Getxo's cemetery gate

The Getxo's cemetery gate, as the malacate building, is already included inside the list of historic and architectural heritage properties from the Basque Country. This gate of the beginning of the twentieth century shows black crusts compactly adhered to sheltered areas of the limestone substrate. It is worth remarking that the gate is situated opposite to the main rainfall direction (see Fig. 1). Three sample fragments of black crust (one of around 2 × 2 and two of around 0.5 × 0.5 cm, respectively) were taken from these areas.

Talaieta street building

This construction is located in Getxo's downtown (Biscay, north of Spain). It was constructed during the last decades of the twentieth century and is one of the typical buildings of the area. It is under the direct influence of road traffic, marine fog, and potential industrial influence. The cantilever does not allow the washing of the zones that it covers, promoting the concentration of soiling in this part, hence in the present work was only regarded the lowest part of the building (at around 1 m above ground level). The damaged façade is constituted by brick-shaped limestones. The limestones with lowest impact show a yellowish color. On the contrary, the most affected ones show a grayish color. The natural yellow hue of the stone is given by the presence of iron as part of its composition. Three fragments of crusts of 3 × 3 (one) and 0.5 × 0.5 (two) cm, respectively, were taken from the grayish affected area.

Instrumentation

SEM-EDS

One sample of each different material and location was selected for the microscopic evaluation. The criteria for the election were both the quantity and the morphology, selecting in this way samples showing the major quantity of crust, and as much flat as possible. All the considered samples were metallized using gold and then studied using an EVO 40 (Carl Zeiss) SEM equipment. The elemental composition of samples was determined by an EDS, using an X-Max (Oxford Instruments) equipment. Data were collected at two different voltages of 20 and 30 keV and a current of 50 μA for the acquisition of images and 200 μA for the acquisition of spectra. The

Fig. 1 **a** Detail of the sampling location, **b** malacate building and detail of its deterioration patterns in sandstone, limestone, and brick (from *right* to *left*), **c** Talaieta street building and a zoom of the soiling process, and **d** cemetery and detail of black crusts on it

working distance ranged between 9 and 11 mm. The EDS spectra were acquired and treated using the INCA software (Oxford Instruments).

The SEM analysis coupled to EDS and processed by the INCA program permits the elemental analysis of selected particles previously seen by SEM. Furthermore, a mapping of specific microscopic areas in the samples is possible, allowing the evaluation of the distribution of these elements over the sample. Additionally, it provides semiquantitative data in terms of weight percentages of the detected elements. It is necessary to underline that the SEM-EDS semiquantitative data provided in this work are just indicative and cannot be considered completely quantitative because no reference materials/standards were used to perform an empirical calibration.

Micro-Raman spectroscopy

For the micro-Raman measurement of biggest crust samples, a Raman Renishaw RA 100 spectrometer, with an excitation wavelength of 785 nm (diode laser) and a Peltier cooled CCD detector, was used for the molecular characterization of the samples. The system was calibrated daily using the 520-cm^{-1} silicon line. In order to avoid thermal decomposition of samples, the laser power (150 mW maximum) was kept in low levels, mainly between 1.5 and 15 mW, depending on the sample.

The spectral resolution was 4 cm^{-1} in the range between 3000 and 200 cm^{-1}, and the spectra were acquired randomly on the crusts under study by accumulating from 5 to 20 scans to improve the signal-to-noise ratio. Due to a microscope lens built in the microprobe (objective lenses of ×4, ×20, ×50) and a video camera, a proper focusing of the laser beam spot is possible (approximately 10–200 μm, depending on the focusing lens). Data acquisition was carried out with the Wire 3.0 software package (Renishaw, UK), and the analysis of the results was performed using the Omnic V.7.2. software (Nicolet).

Additionally, a portable Raman spectrometer (innoRam $B_{\&}WTEK_{INC.}$) was used for the measurement of the smallest crust samples. This spectrometer implements a 785 nm excitation laser source and has a variable power range up to 300 mW. The probe offers also the possibility to perform microscopic analysis mounting it on a micro-camera and using different objective lenses (×20 and ×50) that allow measuring areas of a diameter between 10 and 200 μm. In contrast to the RA 100 spectrometer, with this instrument, samples can be placed under the objective lens to acquire the Raman spectra. With the RA100 spectrometer, samples must be placed vertically on a support to perform the spectral acquisition. This sample positioning could be more difficult for small samples (0.5 × 0.5 cm); thus, it was decided to use the portable innoRam spectrometer available in the laboratory for measurement.

Finally, in the cases where the 785 nm excitation wavelength was giving a weak Raman signal, a 514 nm excitation wavelength (50 mW nominal laser power) was used. With this purpose, an inVia Renishaw confocal Raman micro-spectrometer (Renishaw, Gloucestershire, UK) coupled to a DMLM Leica microscope with a variety of objective lenses (×20, ×50, and ×100) to choose and a Peltier cooled CCD detector which implements a 514-nm excitation wavelength laser was used.

The interpretation of the acquired Raman spectra was carried out by comparison with the Raman spectra of standard samples that are registered in the dispersive Raman spectroscopic database of e-VISNICH (Maguregui et al. 2010a) and comparing with free Raman databases (e.g., RRUFF (Downs and Hall-Wallace 2002)).

Results and discussion

In the Table 1, a summary of the main results obtained for the crust samples of the three buildings located in the municipality of Getxo, in the Bilbao metropolitan area, after the application of the proposed analytical methodology is presented.

Black crust of malacate building

Raman characterization

Gypsum ($CaSO_4{\cdot}H_2O$) was the main constituent identified on the black crusts growing on the three building materials from the malacate building, which can be formed as a consequence of the transformation of calcite ($CaCO_3$) in the presence of atmospheric sulfur oxide (wet or dry deposition) (Morillas et al. 2016d; Morillas et al. 2016e). Moreover, several iron oxides were characterized. Hematite (Fe_2O_3) was found on all three substrates, with major presence in the case of limestone, pointing out the exposure of the building to Fe-rich particles. Moreover, magnetite (Fe_3O_4) was also detected on samples of the black crust on limestone. The size of the magnetite particles identified ranges from 5 to 50 μm. Thus, it can be considered that isolated spherules and agglomerates could be present on the black crusts formed on the limestone. Magnetite can be associated with atmospheric particles in the urban environment. They are mainly derived from combustion processes such as industrial, domestic, and vehicle emissions or from abrasion products from asphalt and from vehicle brake systems (Gautam et al. 2005).

Additionally, Raman spectroscopic analysis performed in black crusts on the brick revealed the presence of a band at 1025 cm^{-1}. Using Raman spectroscopy, it has been proven that iron (III) oxide is present in the original brick composition (see Raman bands related with hematite in Fig. 2a). The band

Table 1 Summary of the main results obtained from the crust sample study

	Malacate sandstone	Malacate limestone	Cemetery gate	Talaieta building
Appearance of the crust	Smooth and compact carbon layer with pores from where the underlying gypsum crystals are observable	Not as smooth and compact carbon layer	A matrix of gypsum crystals with depositions of carbon particles and particles deposited randomly	Brownish crust with not so many gypsum crystals and several randomly arranged particles without cohesion
Main components	Gypsum Amorphous carbon Hematite	Gypsum Amorphous carbon Hematite Magnetite	Gypsum Carotenoids Hematite Magnetite	Gypsum Aluminosilicates
Graffiti remains		Phthalocyanine blue Black diamond Burnt sienna (?)		Ultramarine blue
Nature of the deposited particles	Aluminosilicates Quartz Calcite Gypsum Marine aerosol particles (Na, K, Mg, and Cl)	Aluminosilicates Quartz Calcite Gypsum Particles coming from marine aerosol including (Na, K, Mg, and Cl)	Aluminosilicates Sulfates Marine aerosol particles (Na, K, Mg, and Cl) Metallic particles (Ti, Mn, Fe, and Zn)	Alkali feldspars Quartz Calcite Hematite Magnetite Carbonaceous particles Marine aerosol particles (Na, K, Mg, and Cl) Fluorine Metallic particles (Ti, Cr, V, Mn, Fe, Cu, Zn, Pb)

at 1025 cm^{-1} can be related with (para)coquimbite ($Fe_2(SO_4)_3{\cdot}9H_2O$), which is a degradation compound formed due to the attack of sulfuric acid aerosol (sulfur dioxide wet deposition) to iron oxides (Maguregui et al. 2011). The atmospheric sulfur oxides (SO_X) usually react firstly with the ions of calcium providing gypsum, and later, this gypsum starts reacting with the iron oxides providing (para)coquimbite, following the reactions (1) and (2) (Maguregui et al. 2010b).

$$H_2SO_4+CaCO_3+H_2O \rightarrow CaSO_4{\cdot}2H_2O_{(s)}+CO_{2(g)} \rightleftarrows CaSO_4 \rightleftarrows Ca^{2+}+SO_4^{2-} \quad (1)$$

$$Fe_2O_{3(s)}+3H^{+}+3HCO_3^{-}+3SO_4^{2-}+3Ca^{2+}+6H_2O \rightleftarrows Fe_2(SO_4)_3{\cdot}9H_2O + 3CaCO_3 \quad (2)$$

According to this reaction, it is supposed to be normal to find (para)coquimbite together with gypsum and hematite, as they are the reactants of this degradation product (see the spectra in the Fig. 2a).

It is very difficult to distinguish among Raman spectra of coquimbite and paracoquimbite, because they are quite similar. Both are iron (III) sulfate non-hydrates and they are also polytypes (a special kind of polymorphism, in which the two polymorphs differ only in the stacking of identical two-dimensional sheets or layers).

The Raman band at 1025 cm^{-1} can be also related with γ-anhydrite (γ-$CaSO_4$) (Wein et al. 2014). In the same spectrum where this band was identified, the main band of gypsum is also present (see Fig. 2a). This observation could also suggest that gypsum is suffering a dehydration process, giving rise to the anhydrous form. Anhydrite is usually crystallized as β-anhydrite. According to some authors, the environmental temperature and the internal stress of the material could have influence in the dehydration process of gypsum, causing the crystallization of the β or γ-anhydrite phase (Comodi et al. 2012; Prieto-Taboada et al. 2014).

The calcite ($CaCO_3$) identified in the brick can arise from the carbonation process of the hydrated calcium oxide ($Ca(OH)_2$), present in the brick, which can be subsequently sulfated (Maguregui et al. 2009). Calcite can also be present as a

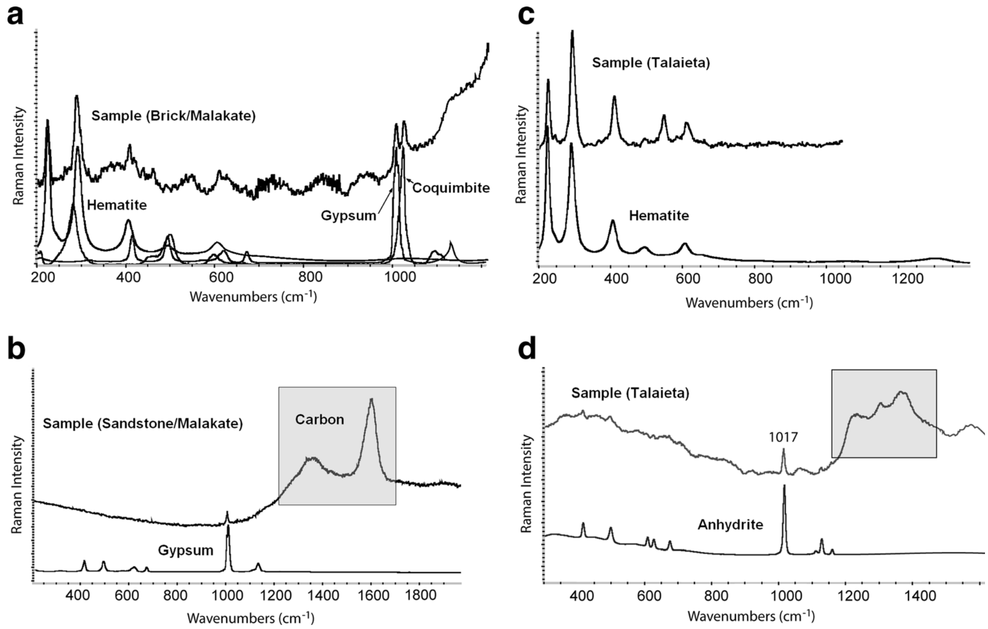

Fig. 2 Raman spectra of samples of **a** malacate's brick showing hematite, gypsum, and (para)coquimbite or γ-anhydrite, **b** malacates's sandstone showing carbon and gypsum, **c** Talaieta street's building showing hematite, and **d** Talaieta street building showing anhydrite

consequence of its deposition on the brick as airborne particulate matter. Unfortunately, it has not been possible to identify calcite on the surface of the brick. Another calcium source could be the remnant calcium carbonate, which has not been completely decomposed into calcium oxide (CaO) during the firing process of the clay from the brick.

Furthermore, several spectra of amorphous carbon were acquired both from the limestone's and sandstone's black crusts. The literature reports that in the carbonaceous content appearing in the black crusts, the organic carbon fraction is usually higher than the elemental fraction in most cases due to a great number of microscopically detectable microorganisms and carbonaceous particles from the atmosphere including organic compounds bound in the surface layer (aliphatic hydrocarbons, polycyclic aromatic hydrocarbons, terpenoid derivatives, etc.) (Saiz-Jimenez et al. 1991; Bonazza et al. 2007).

Additionally, the presence of other compounds, coming from anthropogenic sources, was also identified in the black crusts from limestone. These are phthalocyanine blues, a phthalocyanine (C_{32},H_{18},N_8)-based compound, widely used in the dying industry. Black diamond pigment, based on carbon black pigment, was also detected. Both are commercial pigments and were ascribed to graffiti residues. Through Raman spectroscopy, burnt sienna was also identified. This is an earth pigment that takes its name from the heated version of raw sienna which contains iron oxide and manganese oxide (Genestar and Pons 2005). Nevertheless, the origin of burnt sienna is not completely clear, since this could be a constituent of the limestone as well, since they are similar from the mineralogical viewpoint.

SEM-EDS evaluation

In the black crust samples from malacate building sandstone, a smooth and compact carbon layer with some pores from where the underlying gypsum crystals are observable can be appreciated (see Fig. 3a, b). Furthermore, depositions of Al-silicates, quartz (α-SiO_2), calcite, and those ascribed to sea aerosol containing Na, Mg, K, and Cl were characterized on the surface. Concretely, in Fig. 3c, a Cl particle inserted in the pores of the carbon layer of the black crust can be observed (see Fig. 3c, d). These finding evidences that the particles coming from the marine aerosol can be deposited and trapped in the black crust matrix (Morillas et al. 2016a).

With regard to the limestone's black crust, carbon was not present as a smooth and compact layer (see EDS carbon map in Fig. S1 from Supplementary Material) like in the black crust from sandstone. In this case, the contribution of calcite depositions ascribed to the crustal particulate matter was observed over calcite crystals, which seemed to have been recrystallized during the black crust formation. In Fig. 4, examples of particles deposited on the black crust can be observed. According to the semiquantitative information included in Table 2 and EDS spectral evidences presented in Fig. 4, not only individual particles of gypsum (see EDS Fig. 4b and Table 2) and calcite (see Fig. 4c and Table 2) were identified on the limestone's black crust but also aggregate particles

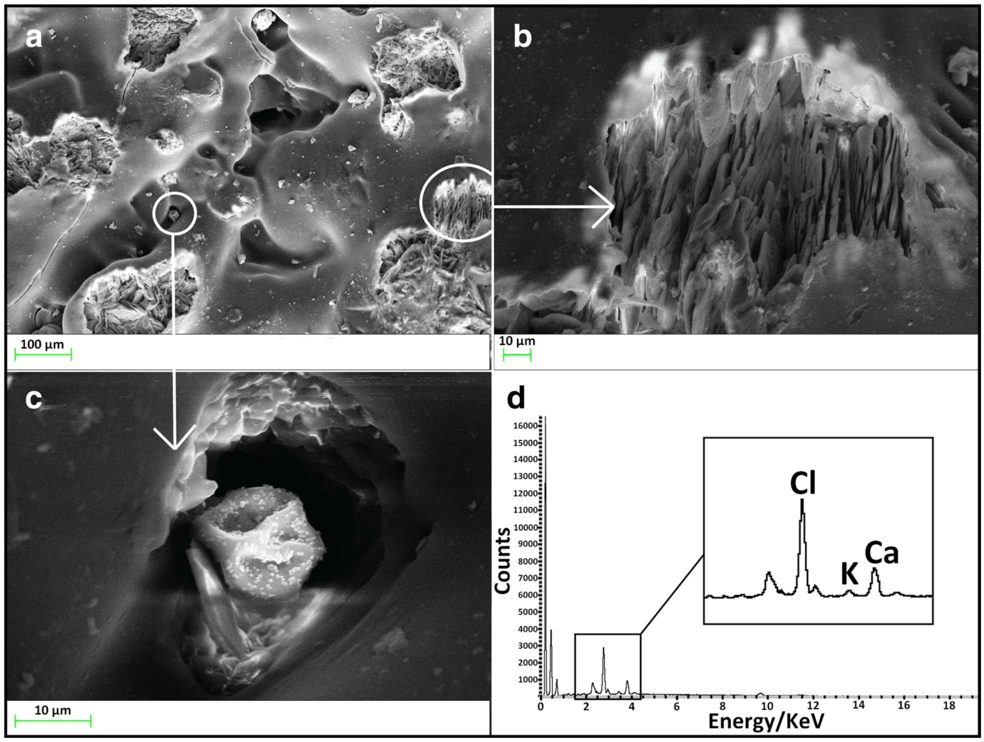

Fig. 3 **a** SEM images of black crust on malacate's sandstone showing a matrix of carbon layer. **b** Zoom of gypsum crystals on the pore. **c** Zoom of a deposited particle. **d** EDS spectrum depicting the main composition of Cl particle in **c**

including aluminosilicates, sulfates, and chlorine (see Fig. 4a and Table 2)

Black crusts of the cemetery gate

Raman characterization

Raman spectroscopy allowed the identification of gypsum, hematite, and magnetite as the main components of the black crusts from the cemetery gate. Gypsum crystals and hematite particles are distributed to a great extent in the black crust, indicating that this building has been influenced by a highly polluted environment. Additionally, carotenoids were also identified embedded in the black crusts, indicating that microorganisms are included inside the matrix of the black crust. These colonizers are able to excrete organic pigments, called carotenoids, or they can be present in its biological structure. Only having the two main Raman bands of carotenoids, it is quite difficult to ascribe this Raman signal to a specific carotenoid, but as it is shown in Fig. S2 from Supplementary Material, this signal could belong to β-carotene.

SEM-EDS evaluation

The black crust in the cemetery gate was constituted by a matrix of gypsum crystals with depositions of carbon and random particles (see Fig. 5b, where the carbon layer is highlighted in red). According to the literature, this is the most characteristic case of black crust (Moropoulou et al. 1998). The average size of the acicular gypsum crystals of the matrix (see Fig. 5a) is circa 30-μm long and 5-μm wide.

Apart from the ubiquitous gypsum, EDS analysis performed on different particles deposited on the gypsum matrix showed that most of the particles consist mainly of aluminosilicates of Ca and K (see Fig. 5c). These compounds can come from the physical and chemical weathering of soils and rocks, then being transported by the wind and finally been deposited in the façades. In atmospheric geochemistry, this kind of compounds is known as crustal particulate matter (Querol et al. 2011) and comprises the 44 % of global emissions of particulate matter (PM) to the atmosphere (Inza-Agirre 2010). Some of the particles (see particle 2 in Fig. 5c) show the presence of S and Cl apart from aluminosilicates and most of them also contain traces of metals such as Fe, Zn, Ti, and Mn (see Fig. 5c). Elements like S (from sulfates) and Cl (from chlorides) can come from particles emitted by marine aerosol (Morillas et al. 2016e). The first element linked with sulfates can come also from anthropogenic emissions or also from calcium carbonate crustal particles that can be transformed in the atmosphere into sulfates by reaction with the H_2SO_4 (coming from SO_X emission) present in the acid rain (Morillas et al. 2016e).

The length of the particles varies in the range of 5 to 15 μm approximately. Apart from the hazards that the pollutants can cause to the human health due to their toxicity (e.g., heavy metals), their size can be also crucial as far as the hazardousness is concerned; the smaller the particles are, the worse is the effect caused on human health. The PM_{10} particles (those

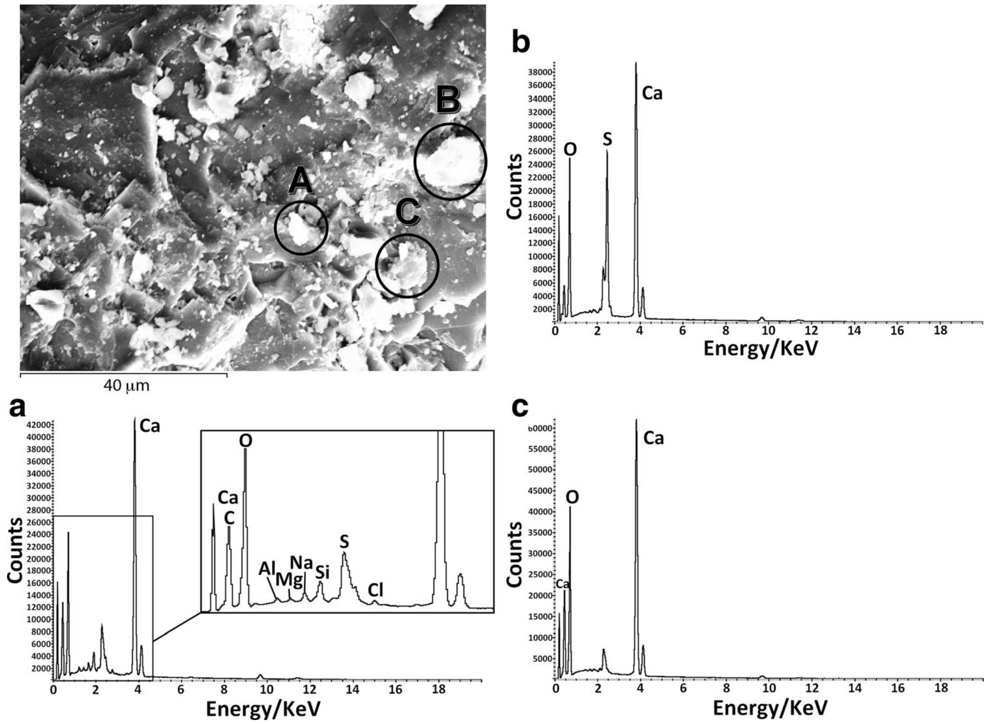

Fig. 4 SEM image of the black crust on malacate's limestone where the EDS punctual analyses were carried out, showing an aggregate of salts (**a**), gypsum (**b**), and calcite (**c**)

sizing less than 10 μm) are more hazardous than the bigger ones, since they are difficult to expel (especially from the human body). Moreover, the particles below 2.5 μm ($PM_{2.5}$) are even more hazardous, since, once inhaled, they reach directly the blood system (Inza-Agirre 2010; EPA 2016).

The composition of particle 4 in Fig. 5a is given in the pie chart (Fig. 5d). It gives an idea of the nature of this kind of aggregates deposited on the surface. Apart from the elements mentioned before, here we can see the contribution of Na, Cl, and Mg, ascribed to the chlorides coming from marine fog.

This is an example of how airborne particulate matter in form of deposition is mixed with particles from both anthropogenic and natural sources. It cannot be predicted if the aggregate has been formed in the atmosphere or once deposited on the gypsum matrix. Nevertheless, the airborne particulate matter tends to sediment once it has reached the aerodynamic diameter of 20 μm. Indeed, the particles with higher diameter are called sedimentable particles and they are characterized by their short time in the atmosphere, which is of about some hours (Inza-Agirre 2010). Therefore, either the source is in the proximity of the building or it has been formed once deposited, acting as a nucleation point.

Soiling process of the Talaieta street building

Raman characterization

A big variety of compounds were identified in this building's samples through Raman microscopy. The presence of iron oxides such as hematite (see Fig. 2c) and magnetite, detected in abundance, was ascribed to the deposition of particulate matter. Silicates, among them quartz and feldspars, such as adularia and sanidine alkali feldspars ($KAlSi_3O_8$), were also identified as particulate matter deposition and more specifically as crustal particular matter. The bands between 1200 and 1600 cm^{-1} in Fig. 2d were initially ascribed to silicates in general, but there is an open discussion about the topic, and the latest assumptions are that they might be fluorescence signals arising from impurities that are actually in silicate matrices but not directly resulting from silicates (Gómez-Nubla et al. 2013). In fact, in a measurement acquired with a 532 nm laser, they should not appear for this same reason.

Degradation products deriving from the interaction between atmospheric pollutants and the calcareous stone surface were also identified, such as gypsum and anhydrite (see Fig. 2d). The presence of calcium sulfates with different hydration states could suggest that the hydration/dehydration cycle of gypsum-anhydrite is taking place (in this case, bassanite was not identified). This cycle produces tension in

Table 2 Semiquantitative composition (% weight units) of deposited particles (see Fig. 4) on the black crust of limestone from malacate building obtained by means of EDS

Spectrum	C	O	Na	Mg	Al	Si	S	Cl	Ca	Fe
A	25.9	61.1	0.3	0.1	0.3	0.6	0.1	0.2	11.1	0.01
B	19.5	64.1					5.4		11.0	
C		85.0							15.0	

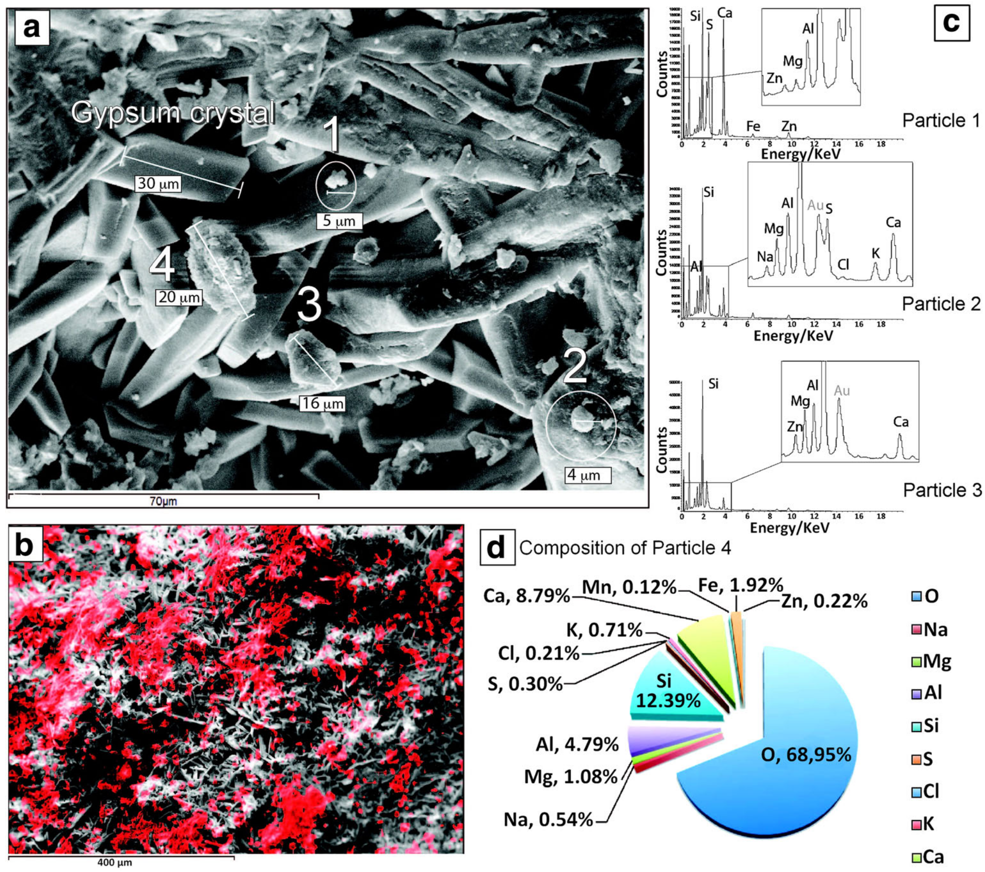

Fig. 5 **a** SEM image of the cemetery gate's black crust showing random depositions. **b** Carbon EDS map highlighted in *red* (**c**). EDS spectra of selected particles on **a** and **d** the pie chart of semiquantitative information about the composition of aggregate particle 4 obtained by EDS

the material due to a volume change on the stone and can promote cracks, fissures, and fractures on the material.

Apart from the exogenous compounds ascribed to degradation processes and atmospheric depositions, some remains of graffiti painting were found. For instance, the presence of ultramarine blue pigment was confirmed by Raman spectroscopy (see Fig. 2a).

SEM-EDS evaluation

At a first stage, the brownish crust present in the Talaieta street building is formed by several randomly arranged particles which do not show strong cohesion as in the rest of the buildings. In this case, there is not an evident gypsum crystals layer. In Fig. 6a, b, Ca, Si and S EDS maps can be observed. As can be appreciated in the overlaid EDS map, Ca is spread over the sample whereas there is predominance in S over Si matching with Ca map. Considering this, it is assumed that the crust is a mixture of gypsum and silicates.

Different subtractions were made on the same EDS maps (in Fig. 5a, b) revealing spots with high amount of Ca, which did not match neither with S nor with Si. Therefore, they were ascribed to possible calcite depositions. Furthermore, several Si accumulation points were also spotted depicting possible quartz depositions. The assumption of being deposited rather than belonging to the substrate is made taking into account the minimum penetration depth of the X-ray beam of the EDS.

EDS spectra indicate a high input of metallic airborne particulate matter. Al, Ca, Fe, K, Ti, Zn, Cu, Pb, Cr, Mn, and V were identified. Among them, titanium particles were the most abundant, regularly accompanied by Fe and traces of Pb and V (see Fig. 6f).

Apart from the Al-silicates encountered repeatedly among the EDS analysis, EDS spectra, acquired on the particle circled in Fig. 6d of more heterogeneous nature and with a diameter of about 3 μm, showed gypsum as one of the main constituents of the particle but also the presence of fluorine (around 22 % in weight). The origin of the fluorine is not clear. Fluorides are naturally occurring components (in rocks, soils, etc.), and they can enter the atmosphere through volcanic emissions and the re-suspension of soil by the wind. Marine aerosols also release small amounts of gaseous hydrogen fluoride and fluoride salts into the air (Franzén 1990; Stefanis et al. 2005). Moreover, it may come from anthropogenic sources such as industry, incinerators, etc. Indeed, fluorine identified on the surface of a building located in Getxo may come from a factory (where fluorine compounds are produced), as has been reported (Martínez-Arkarazo et al. 2007).

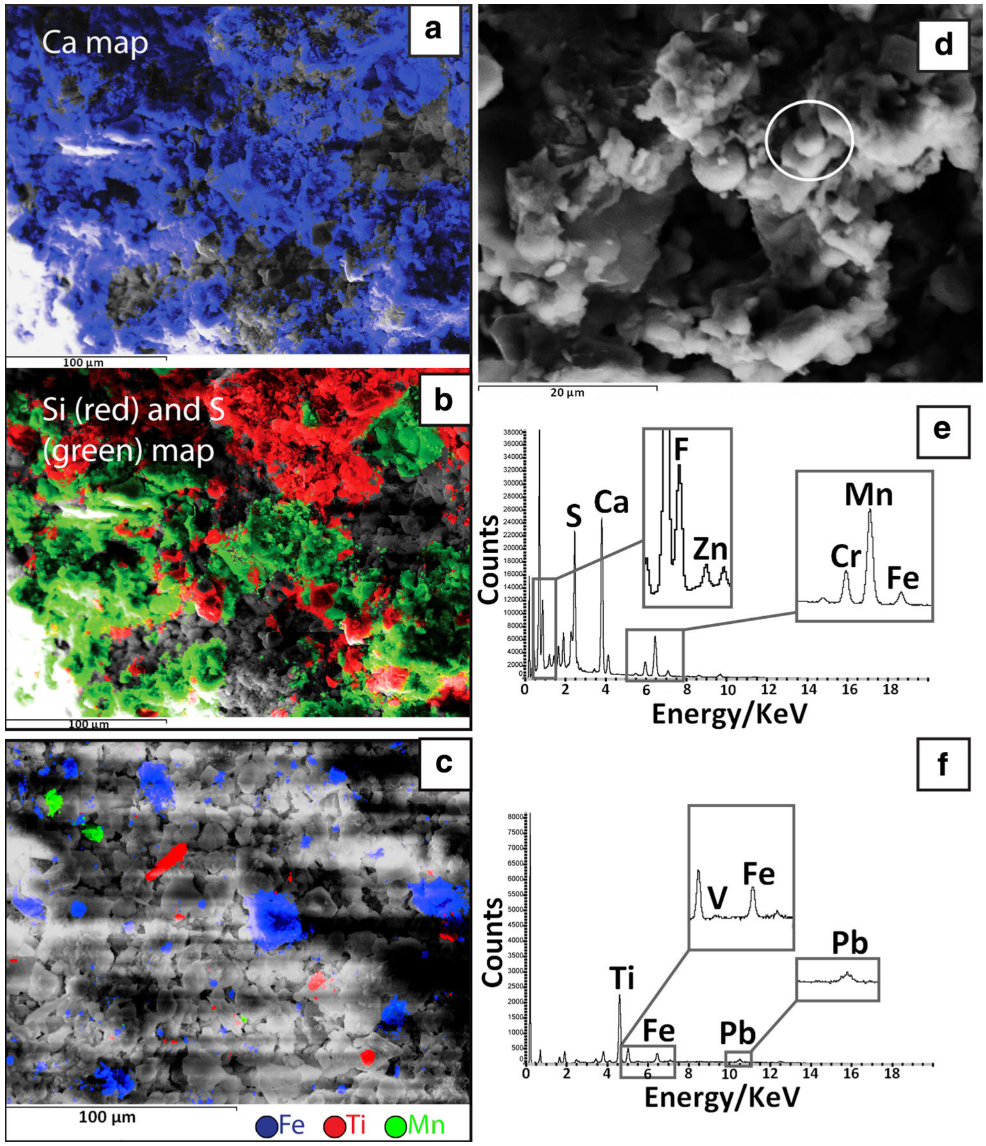

Fig. 6 Soiling-affected samples of Talaieta street building: **a** Ca EDS map, **b** Si and S EDS maps overlapped on the same microscopic area as **a**, **c** metallic particles identified by EDS on the same microscopic area, **d** additional microscopic area focused with the SEM, **e** EDS analysis of the particle circled in **d**, and **f** EDS spectrum of Fe particles from **c**

With regard to the metallic element distribution, the predominant element was found to be iron as is depicted in Fig. 6c (Fe particles are highlighted in blue). This spot was considered as representative of the sample as this behavior is extended along the surface. These maps contribute to know the way in which metallic particles are deposited. At this spot, Mn-, Fe-, and Ti-rich particles are shown. Iron is clearly the most abundant element, being deposited in a wide range of different particle sizes, which range from 1 μm long to a diameter of 20–25 μm approximately. The EDS spectrum of the Fe particle particularly revealed the contribution of other metals such as Zn and traces of Pb (see Fig. 6f).

In addition to Fe, titanium particles with acicular shape of 20-μm long approximately can be observed (see Fig. 6c). And finally, manganese is present in a minor extent with an average size of around 5 μm. The EDS spectrum of the Mn particle revealed that it is composed mainly of Mn, without any contribution of other metals, in contradiction to the cases of other aggregates.

Thanks to the EDS maps, through correlation of the elements, it was possible to evaluate the different kinds of depositions apart from those mentioned before. On the one hand, the influence of marine aerosol is obvious. The EDS maps of Na, Cl, and also Mg are quite coincident, suggesting deposition of halite (NaCl) and MgCl (see Fig. S3 from Supplementary Material). Moreover, in some microscopic areas from the Na and Cl EDS maps, both element distributions are coincident pointing out the presence of halite (NaCl) crystal (see Fig. S3 from Supplementary Material). On the other hand, the depositions of aluminosilicates are shown in the EDS maps of Al and Si (see Fig. S3 from Supplementary Material). Furthermore, the distribution of Fe and Ti highlights again the high rate of metallic depositions on the sample (see

Fig. S3 from Supplementary Material). Finally, the C map showed an accumulation, which indicates the presence of carbonaceous particles, probably corresponding to soot (see Fig. S3 from Supplementary Material).

In order to perform a comparative analysis of the elemental composition from each representative crust extracted from the three buildings, three selected areas from each crust sample (one from each building) were analyzed by EDS. For each crust sample, the semiquantitative information from the three selected areas was obtained and an average value was calculated for each building crust sample. In Fig. 7, a representative SEM image of each building crust sample is shown together with the semiquantitative values (average) obtained from each building crust sample. The results pointed out that the major concentration of sulfur was present in the cemetery gate's black crust. Hence, it is assumed that the limestone of the cemetery has been exposed to an atmosphere rich in SO_x acid aerosols for a longer period of time comparing with the rest of the building, with the proper conditions to commence an important sulfation process, enhancing in this way the formation of crystals that are, doubtless, the best formed crystals comparing to the rest of the samples in terms of size and crystal structure (see SEM image 3 in Fig. 7 showing the sulfate crystals from the cemetery gate's black crust in comparison with the crusts of the other two buildings).

Conclusions

Through the evaluation of the different patterns of weathering processes—all due to atmospheric influence—among the analyzed façades, it was determined that the presence of sulfates was massive in the case of limestone's black crusts and minor in the case of other materials. Despite the minor presence of sulfates, the hazardousness of the identified anhydrite plays a crucial role in the soiling of Talaieta street building due to the dissolution/precipitation processes that can suffer this kind of sulfate.

All the cases showed the influence of marine aerosols, being the case of Talaieta street building the most affected one. In this case, the contribution of marine aerosols may have played a negative role in the formation of the crust (contribution of airborne particulate matter).

Carbonaceous particles associated to the nearby preexisted railway and road traffic were found in a great extent in the crusts formed on the sandstone from the malacate building. These particles have formed a smooth compact layer over the gypsum crystals of the crust.

Regarding the rate of depositions, the most recently constructed building is the most affected by the depositions of airborne particulate matter, depicting the highest susceptibility (among the studied substrates) that has been ascribed to the low quality of the building material associated to the high percentage of aluminosilicates in the substrate.

The malacate construction has been exposed to a polluted atmosphere rich in SO_x and iron particles, as the advanced stages of the crusts indicate the presence of hematite, magnetite, and (para)coquimbite.

The cemetery gate has undergone the formation of a crust, which also hosts microorganisms/colonizers, depicting a complex black crust matrix.

The use of molecular and elemental spectroscopic techniques allowed the determination of the degradation state of the

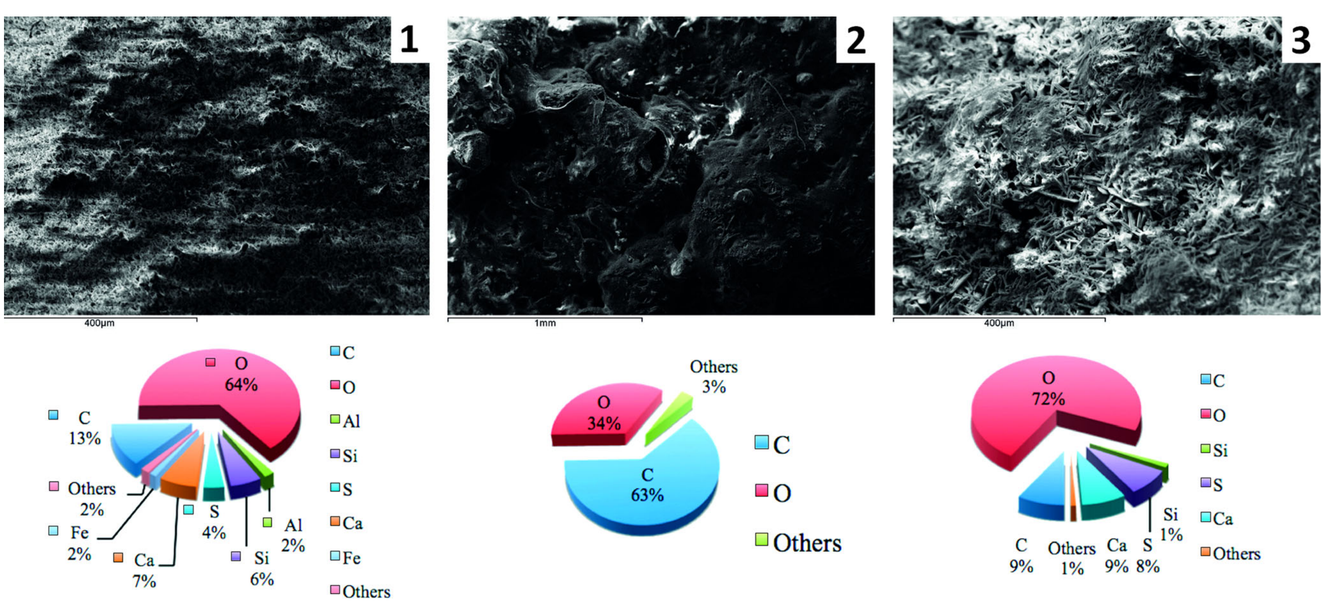

Fig. 7 SEM images and the corresponding semiquantitative composition (atomic %) acquired by EDS analysis. Samples corresponding to the soiling of the building of Talaieta street (*1*), black crust on the sandstone of the malacate (*2*), and on the limestone of the cemetery gate (*3*)

substrates due to the formation of soiling and black crusts. Moreover, micro-Raman spectroscopy together with SEM-EDS has proven to be a reliable combination for the assessment of the depositions of airborne particulate matter and the degradation products formed due to the impact of atmospheric pollutants, as well as any other inputs such as graffiti for example.

The use of micro-Raman spectroscopy results in a valuable resource for this kind of crusts, especially regarding the characterization of crustal particulate matter such as hematite and magnetite, feldspars such as adularia, sanidine, and other kind of Al-silicates as well as calcium sulfates.

Acknowledgements This work has been funded by the Spanish Ministry of Economy and Competitiveness (MINECO) through the project DISILICA-1930 (ref. BIA2014-59124-P) and the Regional Development Fund (FEDER). E. Calparsoro is grateful also to the Spanish Ministry of Economy and Competitiveness (MINECO) who funded his pre-doctoral fellowship (ref. BES-2014-068940). Technical support provided by the Raman-LASPEA laboratory of the SGIker (UPV/EHU, MICINN, GV/EJ, ERDF, and ESF) is also gratefully acknowledged.

References

Barca D, Belfiore CM, Crisci GM, La Russa MF, Pezzino A, Ruffolo SA (2010) Application of laser ablation ICP-MS and traditional techniques to the study of black crusts on building stones: a new methodological approach. Environ Sci Poll Research 17:1433–1447

Barca D, Belfiore CM, Crisci GM, La Russa MF, Pezzino A, Ruffolo SA (2011) A new methodological approach for the chemical characterization of black crusts on building stones: a case study from the Catania city centre (Sicily, Italy). J Anal At Spectrom 26:1000–1011

Barca D, Comite V, Belfiore CM, Bonazza A, La Russa MF, Ruffolo SA, Crisci GM, Pezzino A, Sabbioni C (2014) Impact of air pollution in deterioration of carbonate building materials in Italian urban environments. App Geochem 48:122–131

Bonazza A, Brimblecombe P, Grossi CM, Sabbioni C (2007) Carbon in black crusts from the tower of London. Environ Sci Technol 41: 4199–4204

Brimblecombe P, Grossi CM (2005) Aesthetic thresholds and blackening of stone buildings. Sci Total Environ 349:175–189

Charola A, Pühringer J, Steiger M (2007) Gypsum: a review of its role in the deterioration of building materials. Environ Geol 52:339–352

Comodi P, Kurnosov A, Nazzareni S, Dubrovinsky L (2012) The dehydration process of gypsum under high pressure. Phys Chem Miner 39:65–71

Crupi V, Allodi V, Bottari C, D'Amico F, Galli G, Gessini A, La Russa MF, Longo F, Majolino D, Mariotto G, Masciovecchio C, Pezzino A, Rossi B, Ruffolo SA, Venuti V (2016) Spectroscopic investigation of Roman decorated plasters by combining FT-IR, micro-Raman and UV-Raman analyses. Vib Spectrosc 83:78–84

Doehne E, Price CA (2011) Stone conservation: an overview of current research, Second edn. Getty Conservation Institute, Los Angeles

Downs RT, Hall-Wallace M (2002) 18th General Meeting of the International Mineralogical Association, Edinburgh, Scotland. Programme With Abstracts, 128

EPA 2016 https://www.epa.gov/pm-pollution [last accessed July 2016]

Espinosa-Marzal RM, Scherer GW (2010) Advances in understanding damage by salt crystallization. Acc Chem Res 43:897–905

Flatt RJ (2002) Salt damage in porous materials: how high supersaturations are generated. J Cryst Growth 242:435–454

Franzén, LG (1990) Transport, deposition and distribution of marine aerosols over southern Sweden during dry westerly storms. Ambio 180–188

Gautam P, Blaha U, Appel E (2005) Magnetic susceptibility of dust-loaded leaves as a proxy of traffic-related heavy metal pollution in Kathmandu city, Nepal. Atmos Environ 39:2201–2211

Genestar C, Pons C (2005) Earth pigments in painting: characterisation and differentiation by means of FTIR spectroscopy and SEM-EDS microanalysis. Anal Bioanal Chem 382(2):269–274

Gómez-Nubla L, Aramendia J, Fdez-Ortiz de Vallejuelo S, Castro K, Madariaga J.M (2013) From portable to SCA Raman devices to characterize harmful compounds contained in used black slag produced in electric arc furnace of steel industry. J Raman Spectrosc 44: 1163–1171

ICOMOS, 2008. http://www.icomos.org/en/component/content/article/116-english-categories/resources/publications/261-monumentsasites-xv. [last accessed July 2016]

Inza-Agirre A (2010) Estudio de series temporales y composición química del material particulado atmosférico en distintas áreas del País Vasco. Thesis, Universidad del País Vasco UPV/EHU

Larssen T, Lydersen E, Tang D, He Y, Gao J, Liu H, Duan L, Seip HM, Vogt RD, Mulder J, Shao M, Wang Y, Shang H, Zhang X, Solberg S, Aas W, Okland T, Eilertsen O, Angell V, Li Q, Zhao D, Xiang R, Xiao J, Luo J (2006) Acid rain in China. Environ Sci Technol 40: 418–425

Maguregui M, Sarmiento A, Martínez-Arkarazo I, Angulo M, Castro K, Arana G, Etxebarria N, Madariaga JM (2008) Analytical diagnosis methodology to evaluate nitrate impact on historical building materials. Anal Bioanal Chem 391:1361–1370

Maguregui M, Sarmiento A, Escribano R, Martinez-Arkarazo I, Castro K, Madariaga JM (2009) Raman spectroscopy after accelerated ageing tests to assess the origin of some decayed products found in real historical bricks affected by urban polluted atmospheres. Anal Bioanal Chem 395:2119–2129

Maguregui M, Prieto-Taboada N, Trebolazabala J, Goienaga N, Arrieta N, Aramendia J, Gomez-Nubla L, Sarmiento A, Olivares M, Carrero JA, Martinez-Arkarazo I, Castro K, Arana G, Olazabal MA, Fernandez LA, Madariaga JM (2010a) CHEMCH 1st international congress chemistry for cultural heritage, Ravenna

Maguregui M, Knuutinen U, Castro K, Madariaga JM (2010b) Raman spectroscopy as a tool to diagnose the impact and conservation state of Pompeian second and fourth style wall paintings exposed to diverse environments (House of Marcus Lucretius). J Raman Spectrosc 41:1400–1409

Maguregui M, Knuutinen U, Martínez-Arkarazo I, Castro K, Madariaga JM (2011) Thermodynamic and spectroscopic speciation to explain the blackening process of hematite formed by atmospheric SO2 impact: the case of Marcus Lucretius House (Pompeii). Anal Chem 83:3319–3326

Martínez-Arkarazo I, Angulo M, Bartolomé L, Etxebarria N, Olazabal MA, Madariaga JM (2007) An integrated analytical approach to diagnose the conservation state of building materials of a palace house in the metropolitan Bilbao (Basque Country, North of Spain). Anal Chim Acta 584(2):350–359

McAlister JJ, Smith BJ, Török A (2008) Transition metals and water-soluble ions in deposits on a building and their potential catalysis of stone decay. Atmos Environ 42:7657–7668

Morillas H, Maguregui M, García-Florentino C, Carrero JA, Madariaga JM (2016a) The cauliflower-like black crusts on sandstones: a natural passive sampler to evaluate the surrounding environmental pollution. Environ Res 17:218–232

Morillas H, García-Galán J, Maguregui M, García-Florentino C, Marcaida I, Madariaga JM (2016b) In-situ multianalytical methodology to

evaluate the conservation state of the entrance arch of La Galea Fortress (Getxo, north of Spain). Microchem J 128:288–296
Morillas H, García-Galán J, Maguregui M, Marcaida I, García-Florentino C, Carrero JA, Madariaga JM (2016c) Assessment of marine and urban-industrial environments influence built heritage sandstone using X-ray fluorescence spectroscopy and complementary techniques. Spectrochim Acta B 123:76–88
Morillas H, Marcaida I, Maguregui M, Carrero JA, Madariaga JM (2016d) The influence of rainwater composition on the conservation state of cementitious building materials. Sci Total Environ 542:716–727
Morillas H, Maguregui M, García-Florentino C, Marcaida I, Madariaga JM (2016e) Study of particulate matter from primary/secondary marine aerosol and anthropogenic sources collected by a self-made passive sampler for the evaluation of the dry deposition impact on built heritage. Sci Total Environ 550:285–296
Moropoulou A, Bisbikou K, Torfs K, Van Grieken R, Zezza F, Macri F (1998) Origin and growth of weathering crusts on ancient marbles in industrial atmosphere. Atmos Environ 32:967–982
Potgieter-Vermaak SS, Godoi RHM, Grieken RV, Potgieter JH, Oujja M, Castillejo M (2005) Micro-structural characterization of black crust and laser cleaning of building stones by micro-Raman and SEM techniques. Spectrochim Acta A 61:2460–2467
Prieto-Taboada N, Gómez-Laserna O, Martinez-Arkarazo I, Olazabal MA, Madariaga JM (2014) Raman spectra of the different phases in the $CaSO_4$-H_2O system. Anal Chem 86:10131–10137
Querol X, Moreno T, Alastuey A, Gibbons W (2011) Geoquímica Inorgánica Atmosférica: Elementos Trazadores de Fuentes Emisoras de Contaminantes. Macla 14:143–144
Rodríguez-Navarro C, Doehne E, Sebastian E (2000) How does sodium sulfate crystallize? Implications for the decay and testing of building materials. Cement Concrete Res 30:1527–1534
Ruffolo SA, Comite V, La Russa MF, Belfiore CM, Barca D, Bonazza A, Crisci GM, Pezzino A, Sabbioni C (2015) An analysis of the black crusts from the Seville Cathedral: a challenge to deepen the understanding of the relationships among microstructure, microchemical features and pollution sources. Sci Tot Environ 502:157–166
Saiz-Jimenez C, Garcia del Cura MA (1991) Sulfated crusts: a microscopic, inorganic and organic analysis. In Science, technology and European cultural heritage, N.S. Baer, C. Sabbioni, A.I. Sors, Oxford, UK, Butterworth-Heinemann 527–534
Sarmiento A, Maguregui M, Martinez-Arkarazo I, Angulo M, Castro K, Olazábal MA, Fernández LA, Rodríguez-Laso MD, Mujika AM, Gómez J, Madariaga JM (2008) Raman spectroscopy as a tool to diagnose the impacts of combustion and greenhouse acid gases on properties of built heritage. J Raman Spectrosc 39:1042–1049
Schiavon N, Chiavari G, Fabbri D (2004) Soiling of limestone in an urban environment characterized by heavy vehicular exhaust emissions. Environ Geol 46:448–455
Stefanis A, Theoulakis P, Pilinis C (2005) The decay effects of sea-salt aerosol on the surface of historic buildings. Proceedings of the 9th International Conference on Environmental Science and Technology, Rhodes Island, Greece, pp A1391–A1396
Sýkorová I, Havelcová M, Zeman A, Trejtnarová H (2011) Carbon air pollution reflected in deposits on chosen building materials of Prague Castle. Sci Total Environ 409:4606–4611
Watson JG, Chow JC, Chen LWA (2005) Summary of organic and elemental carbon/black carbon analysis methods and intercomparisons. Aerosol Air Qual Res 5:65–102
Wein J, Wang A, Lambert JL, Wettergreen D, Cabrol NA, Warren-Rhodes K (2014) Mars microbeam Raman spectrometer (MMRS) on-board the Zöe Rover in the Atacama In 11th International Georama Conference St. Louis, USA